

Guiding Competitive Binding Assays Using Protein–Protein Interaction Prediction: The HER2–Affitin Use Case

Published as part of ACS Omega special issue “3D Structures in Medicinal Chemistry and Chemical Biology”.

Anna Ranaudo,* Ugo Cosentino, Claudio Greco, Giorgio Moro, Alessandro Maiocchi, and Elisabetta Moroni



Cite This: *ACS Omega* 2024, 9, 49522–49529



Read Online

ACCESS |



Metrics & More

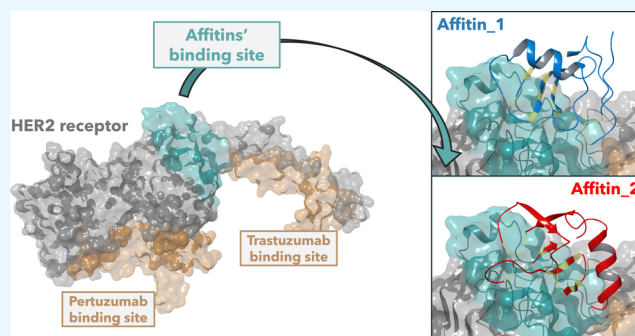


Article Recommendations



Supporting Information

ABSTRACT: Affitins are a class of small artificial proteins, designed as alternatives to antibodies for therapeutic, diagnostic, and biotechnological applications. Recent patents by Bracco Imaging S.p.A have demonstrated the potential of two engineered affitins for designing imaging probes to detect and monitor human epidermal growth-factor receptor 2 (HER2) levels *in vivo*. Targeting HER2 is critical, as its overexpression is linked to poor prognosis of several cancer diseases, making it a key marker for treatment strategies and diagnostic tools. Interestingly, these affitins do not compete with the commonly used monoclonal antibodies trastuzumab and pertuzumab for HER2 binding sites, allowing their concurrent use *in vivo* and making them suitable for imaging or diagnostic purposes. Since these two affitins compete for the same yet unidentified binding site on HER2, structural insights into these interactions are essential for facilitating the design and development of more effective diagnostic tools and treatments. In this study, we used protein–protein docking and molecular dynamics simulations to model the binding of these affitins to HER2. The stability of the predicted complexes was quantified by using the DockQ parameter, a widely used metric for evaluating protein–protein docking predictions. The docking poses were then compared with HER2 sites likely to interact with a protein partner, as predicted by the matrix of local coupling energies method. The combination of these two computational methods allowed for the identification of the most likely docking poses. Comparative analysis with HER2–protein complexes from the Protein Data Bank suggests that both affitins may bind HER2 at the same epitopes as an antibody fragment and an affibody. These findings indicate that targeted competitive binding assays could efficiently reduce the experimental efforts to map the HER2–affitin interactions. The computational approach proposed in this study not only provides insights into this specific case but also establishes a robust framework applicable for facilitating the structural modeling and interaction prediction of other affitin–protein systems.



INTRODUCTION

The receptor tyrosine-protein kinase erbB-2, also known as tyrosine kinase-type cell surface receptor human epidermal growth-factor receptor 2 (HER2), proto-oncogene c-ErbB-2, proto-oncogene Neu, or human epidermal growth-factor receptor 2 (HER2), is encoded in humans by the gene ERBB2 (Uniprot code:P04626).¹ The HER2 receptor, a member of the epidermal growth-factor receptor (EGFR) family of tyrosine kinases, is a mediator of cell proliferation and differentiation in human tissues. If inappropriately activated, HER2 is closely associated with the development and the severity of many tumoral pathologies.² Among these diseases, HER2 is known to be overexpressed in 20–25% of breast cancers.³ Consequently, it is a well-assessed molecular target for both diagnostic and therapeutic purposes.

Common cancer therapies involve the use of monoclonal antibodies (mAbs), such as trastuzumab⁴ and pertuzumab,⁵

which have now been approved since more than two and one decade, respectively; they are also used in combination.⁶ The crystal structures of their antigen-binding fragments (Fab) with the extracellular domain (ECD) of HER2 have been determined through X-ray diffraction^{2,7} and have been deposited in the Protein Data Bank (PDB), giving insights into the mechanisms of action toward the target. The cryo-EM structure of the HER2–trastuzumab–pertuzumab complex is available too.⁸

Received: August 9, 2024

Revised: November 19, 2024

Accepted: November 22, 2024

Published: December 5, 2024



Despite being well-assessed targeting agents, mAbs suffer from several drawbacks; these are mostly related to their size, which causes a difficult penetration in the tissues and a complicated production, due to the many domains they are composed of. For these reasons, attention has been shifted to the use of mAbs fragments, such as antigen-binding fragments (Fab), single-chain variable fragments (scFv), diabodies, triabodies, minibodies, and single domain antibodies (sdAb).⁹ As the use of these fragments still presents some limits,¹⁰ small-sized, stable, synthetic proteins that are referred to with the term “antibody mimetics,” have also been taken into account.^{9,10} These alternatives to the mAbs-based scaffolds have been considered for targeting HER2 too, and several examples can be found in the recent literature, which include, e.g., an affibody,¹¹ a designed ankyrin repeat protein (DARPin),¹² and a repebody.¹³

In the category of the antibody mimetics, affitins, 7 kDa-proteins engineered from the wild-type DNA-binding protein Sac7d,¹⁴ can be included as well. These proteins have been studied for their interesting properties such as high tissue penetration potential and the conservation of the exceptional biophysical features of the wild-type, i.e., resistance to temperature (up to 90 °C) and pH (0–13). A quite recent application foresees the employment of an affitin for the recognition of the molecular target epidermal growth-factor receptor (EGFR).¹⁵

Recently, two patents have been published by Bracco Imaging S.p.A.^{16,17} in which two affitins (Affitin_1 and Affitin_2 from now on) have been engineered, through the full randomization of 14 residues responsible for the interaction with the DNA in the wild type, in order to achieve a high binding affinity toward HER2. Competitive binding assays have shown that both affitins recognize HER2 at specific epitopes—which are at least partially overlapping—distinct from those recognized by the mAbs trastuzumab and pertuzumab.^{16,17} This suggests that Affitin_1 and Affitin_2 could be used, upon appropriate functionalization, which is also object of the patents,^{16,17} as molecular probes for the detection of HER2 concurrently with a trastuzumab- or pertuzumab-based therapy. This could give the possibility of monitoring HER2 levels during therapy, thus evaluating the effectiveness of the latter.

Although it is known that both affitins bind HER2, the structures of HER2–affitin complexes have not yet been determined. However, gaining structural insights into these interactions would be essential for the comprehension of the binding mechanisms, which can in turn help, e.g., in the optimization of the binding affinity.

Well-known methods for the study of protein–protein interactions, e.g., X-ray diffraction and nuclear magnetic resonance, require the preparation of adequate samples and are time-consuming and expensive. For these reasons, *in silico* approaches such as molecular docking are widely used for a rapid, preliminary prediction of the three-dimensional structure of a protein–protein complex. Despite being well-assessed methods, the accuracy of a docking prediction is nowhere near the one that can be achieved with experimental methods. From this, two consequences arise. First, if some experimental evidence is available, then it must be used for driving the prediction. Second, what results from the *in silico* prediction should be used for guiding further experiments rather than to be taken as a definitive result. The second point is particularly true when docking results are concerned as they

consist in an ensemble of poses often characterized by similar scores; in other words, they are equally likely. A “post-docking” procedure, aimed at the rescoring of the docking poses, is thus necessary. The selection of a subset of all the possible poses, extracted thanks to the “post-docking” stage, can then be used for performing targeted experimental tests.

The aim of this study is to gain a deeper understanding of the binding between Affitin_1 and Affitin_2 to the receptor HER2. For this purpose, docking calculations have been carried out by exploiting the experimental information at our disposal, i.e., the lack of competition toward the binding of HER2 between the affitins and the mAbs trastuzumab and pertuzumab, and the awareness that the mutated residues of the affitins are the most relevant for the interaction. In the second part of the study, the considerations we made in a previous work¹⁸ have been applied for finding out which are the more likely docking poses. In brief, the poses were evaluated by two different approaches. The first one consists in the evaluation of their stability along molecular dynamics (MD) simulations; the stability is quantified with the calculation of the DockQ parameter.¹⁹ The second approach consists in the comparison of the poses with HER2 patches predicted to be able to bind a protein partner; that prediction was made with the matrix of local coupling energies (MLCE) method.^{20–23} Finally, the subset of docking solutions selected with DockQ and MLCE was compared with the HER2 sites that are experimentally known to be responsible for the interaction with other protein partners. Thanks to this comparison, two of the many interactors of HER2 were selected for future competitive binding assays, thus reducing the time and the costs required for carrying out the experiments.

METHODS

Preparation of the Input Files. The structure of the Affitin_1 and Affitin_2 have been prepared starting from their sequences, stated in the patents^{16,17} and shown in [Supporting Figure S1](#). A homology modeling procedure has been used, using a tool included in Bioluminate [Schrödinger Release 2023–3: BioLuminate, Schrödinger, LLC, New York, NY, 2023] and by setting as a template the three-dimensional structure of the wild-type affitin Sac7d (PDB ID:1AZQ). Molecular dynamics (MD) simulations of the generated models and of Sac7d have then been carried out to evaluate the conservation of the fold of the wild-type affitin following the introduction of the mutations. Simulations have been performed with Gromacs (release 2020.6)²⁴ and the united atom Gromos 53A6 force field²⁵ together with the SPC water model.²⁶ Following energy minimization and solvent equilibration, three independent 300 ns production runs were performed at constant temperature (300 K) and pressure (1 bar). Analysis, performed for each affitin on the three concatenated trajectories, include clustering of sampled conformations; calculations of the root-mean-square fluctuations (RMSF) of backbone atoms; calculation of the fraction of secondary structure. Further details about the MD simulations and their analysis are shown in [Supporting Text S1](#). MD simulations of the affitins were carried out with the all-atom AMBER99SB-ILDN force field²⁷ too, to ensure that the results obtained were not strongly dependent on the chosen force field. These simulations were conducted with the same setup used for those with the Gromos 53A6 force field; however, the

TIP3P water model²⁸ was used, as it is the one used in the development of the AMBER99SB-ILDN force field.

The three-dimensional structure of receptor HER2 was retrieved from the PDB (PDB ID:6OGE). The structure file was processed with the Protein Preparation Wizard²⁹ [Schrödinger Release 2023–3: Protein Preparation Wizard; Prime, Schrödinger, LLC, New York, NY, 2023] to remove water molecules and counterions, add hydrogen atoms and other potentially missing atoms, rebuild missing side chains and loops, optimize the hydrogen bonding network, and perform energy minimization of hydrogen atoms. This prepared crystallographic structure was then used for docking calculations.

Additionally, MD simulations were conducted for the complex HER2-trastuzumab to obtain a number of conformations for the subsequent MLCE prediction (see paragraph MLCE-based prediction of HER2 binding sites). The rationale for performing simulations in the presence of the mAb trastuzumab is related to the large displacement observed in domain IV of the receptor during MD simulations of the receptor alone (data not shown); this displacement was absent when the mAb was bound. The simulations were performed using the GROMOS 53A6 force field with the same setup used for the affitins, except that three replicas, each 100 ns in length, were performed.

Docking Calculations. Protein–protein docking calculations have been carried out with the web server ClusPro.^{30–32} The structures of the affitins and HER2 prepared as previously stated were uploaded as “ligand” and “receptor,” respectively. The “balanced” scoring scheme has been employed. The experimental information is exploited as follows. An attractive potential has been applied on the 14 mutated residues of the affitins (see Supporting Figure S2), in such a way to drive the docking prediction toward poses having those residues part of the affitin–HER2 interface. As for the receptor, the residues within 10 Å from the mAbs trastuzumab and pertuzumab were masked during the calculation (see Supporting Figure S3), to satisfy the experimental evidence that the affitins bind HER2 on different epitopes. The docking models were visually inspected, and a subset of them was selected for further analysis (see Results and Discussion—Docking Calculations).

DockQ Evaluation of the Quality of the Docking Models. MD simulations were performed on the selected docking models, following the approach proposed by Jandova and co-workers³³ which suggests that near-native models, i.e., models closer to the true structure of the complex, should be more stable during the simulations with respect to non-native models. Details of the setup of the MD simulations are shown in Supporting Text S2.

The stability, and thus the quality of the models, was evaluated through the calculation of the parameter DockQ¹⁹ along the MD trajectories. DockQ originates from the three CAPRI parameters³⁴ interface-RMSD (i-RMSD), ligand-RMSD (l-RMSD), and fraction of native contacts (Fnat). The average values of three parameters i-RMSD, l-RMSD and Fnat are calculated from MD trajectories every 500 ps, and the DockQ values are thus evaluated. DockQ ranges from 0 to 1: high-quality models are defined by $\text{DockQ} \geq 0.80$, medium-quality for $0.80 > \text{DockQ} \geq 0.49$, acceptable-quality for $0.49 > \text{DockQ} \geq 0.23$, and models are incorrect if $\text{DockQ} < 0.23$. The CAPRI parameters and the DockQ were calculated along the MD simulations with respect to the starting structure of the simulation, which corresponds to the docking pose after energy

minimization and short NVT and NPT equilibrations stages, performed as in Supporting Text S2.

MLCE-Based Prediction of HER2 Binding Sites. The matrix of local coupling energies (MLCE) method^{20–23} was employed for the prediction of HER2 areas that are more likely to bind a partner (from now on, patches), and thus affitins too. This approach combines the analysis of a given protein's energetic properties with that of its structural determinants, based on the idea that some residues stabilize the protein fold, while others, less energetically coupled to the protein itself, may interact with a partner. The calculations have been carried out with the program REBELOT, version 1.3.2 (<https://github.com/colombolab/MLCE>) on the centrotypes of 4 clusters (Supporting Figure S4) which cover around 90% of the conformation variability of HER2 sampled during three MD simulations (100 ns each). The patches were predicted on the crystal structure of HER2 (PDB ID:6OGE, the same used for docking calculations) by considering the top 15% of spatially contiguous residue pairs with the lowest-energy interactions.

RESULTS AND DISCUSSION

Structure Prediction of Affitin_1 and Affitin_2. The wild-type affitin Sac7d and the homology models of Affitin_1 and Affitin_2 were subjected to MD simulations (three 300 ns replica each). Convergence of MD simulations was checked by looking at the root-mean-square deviations (RMSD) of backbone atoms (Supporting Figure S5). All the analyses were conducted on the three concatenated trajectories as specified in Supporting Text S1. The most representative conformations of the affitins in aqueous solution, i.e., those more frequently sampled during the simulations, were retrieved by a cluster analysis (0.4 nm cutoff). The centrotypes of the clusters were then visually inspected. It can be observed that (i) the fold of Sac7d in aqueous solution is almost entirely conserved with respect to the crystallographic structure; (ii) the fold of the two engineered affitins is mostly identical to the wild-type affitin fold (Figure 1).

The calculation of the fractions of secondary structure elements confirms the similar behavior of the three affitins in aqueous solution. The engineered affitins, Affitin_1 and Affitin_2, exhibit minor differences compared to the wild-type Sac7d, being slightly less structured (sum of secondary structure elements: 67 and 65% respectively, compared to 73%

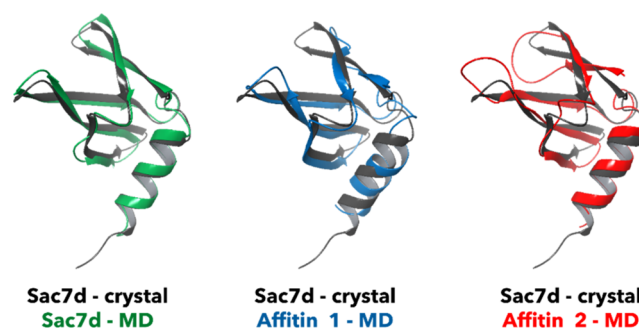


Figure 1. Superposition of the centrotypes of the most populated clusters obtained from the MD simulations (GROMOS 53A6 force field) of the wild-type affitin Sac7d (green), Affitin_1 (blue), and Affitin_2 (red) onto the Sac7d crystallographic structure (PDB ID: 1AZQ, in black). The populations of the most populated clusters are 75, 79, and 87% for Sac7d, Affitin_1, and Affitin_2 respectively.

Table 1. First Ten Docking Poses for Affitin_1 and Affitin_2, by ClusPro Ranking^a

ClusPro ranking		Num. of clusters members		Mutated affitins' residues in contact with HER2	
Affitin_1	Affitin_2	Affitin_1	Affitin_2	Affitin_1	Affitin_2
#0	#0	131	92	14	14
#1	#1	110	85	12	14
#2	#2	68	66	13	14
#3	#3	64	54	14	11
#4	#4	52	54	10	12
#5	#5	49	53	14	9
#6	#6	47	53	13	13
#7	#7	46	50	12	13
#8	#8	45	42	12	7
#9	#9	42	41	12	9

^aFor the first ten docking poses, the ClusPro ranking, the number of cluster members, and the number of the mutated affitins' residues in contact with HER2 (within a cutoff of 5.5 Å) are shown. The color of the rows indicates the binding areas on the receptor (red, yellow, orange, and green).

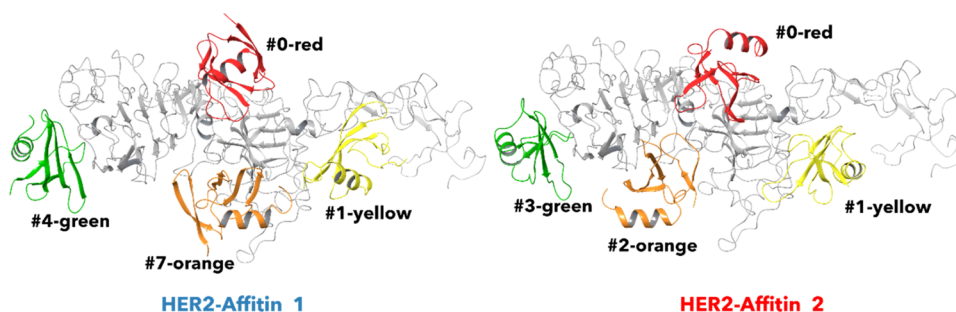


Figure 2. Superimposition of the four HER2–Affitin_1 (left) and the four HER2–Affitin_2 (right) best scoring docking models for each binding area (red, yellow, orange, and green). Affitins are colored based on the binding area and labeled with “#ClusPro ranking-colour”. HER2 is shown in gray. The docking models shown in this figure are selected for the DockQ and MLCE evaluations.

of Sac7d). All values are reported in Supporting Table S1. The similarities among the three affitins are also evident from the RMSF values of the backbone atoms. All three affitins show higher RMSF values at the terminal, α -helix, and interstrands residues (see Supporting Figure S6). Overall, the introduction of mutations into the sequence of the wild-type affitin Sac7d does not affect the fold, which is conserved in both mutated affitins. Simulations performed with the AMBER99SB-ILDN force field produced comparable RMSD and RMSF values (Supporting Figures S5 and S6) as well as secondary structure elements (Supporting Table S1). Given the similar results obtained with both force fields, the computationally cheaper Gromos 53A6 force field was selected for the simulations of the receptor and HER2–affitins docking poses.

Docking Calculations. Docking calculations carried out with ClusPro, guided by the experimental information available, resulted in 27 and 28 models for the partners HER2–Affitin_1 and HER2–Affitin_2, respectively, out of a maximum of 30 that ClusPro can provide. They were visually examined by superimposing them on each other on the receptor structure. Both Affitin_1 and Affitin_2 appear to bind to only four different areas of the HER2 receptor. These areas are highlighted by coloring the affitins in red, yellow, orange, and green (Supporting Figure S7). Table 1 shows, for both affitins, the first ten docking models by ClusPro ranking, which is based on the population of the clusters; the binding areas (red, yellow, orange, and green) for each docking model are also shown.

For the evaluation based on DockQ and MLCE, the best scoring models of each area for Affitin_1 and Affitin_2 were

selected from all of the obtained models. The selected models, shown in Figure 2, are labeled by their ClusPro ranking and the color indicating the binding area. For Affitin_1, the selected models are #0-red, #1-yellow, #4-green, and #7-orange. For Affitin_2, the selected models are #0-red, #1-yellow, #2-orange, and #3-green.

DockQ-MLCE Evaluation of the Docking Models. The four models of each affitin were subjected to MD simulations, and the DockQ parameter was calculated along the trajectories. In parallel, an MLCE calculation was performed on representative conformations of HER2. The docking models were compared with the patches by visual inspection and by calculating the number of HER2 residues belonging to a patch and involved in the docking solutions. The decision on which docking models are most likely should be made on the basis of the two combined approaches, i.e., possibly seeking a consensus between the two. It is important to remark that DockQ and MLCE rely on totally different assumptions. Indeed, the MLCE method analyzes protein energetics to identify potential binding sites on protein surfaces, focusing on regions minimally coupled to the rest of the structure. It is based on the observation that epitopes, recognized by binding partners like antibodies, are mutation-tolerant, flexible, and accessible on the protein surface and thus do not significantly stabilize the protein's fold. Based on this assumption, MLCE evaluates residue–residue interactions by constructing a matrix of average nonbonded interaction energies from molecular dynamics simulations, which is then simplified using eigenvalue decomposition to identify strong and weak interaction sites. Low-intensity couplings suggest protein areas that are

Table 2. ClusPro Rankings, DockQ Scores, and MLCE Values of the Selected Docking Poses of Affitin_1 and Affitin_2 with HER2^a

Docking area	ClusPro ranking		DockQ		MLCE	
	Affitin_1	Affitin_2	Affitin_1	Affitin_2	Affitin_1	Affitin_2
Red	#0	#0	0.45 (medium)	0.37 (acceptable)	3	9
Yellow	#1	#1	0.27 (acceptable)	0.29 (acceptable)	27	27
Green	#4	#3	0.31 (acceptable)	0.19 (incorrect)	0	0
Orange	#7	#2	0.33 (acceptable)	0.38 (acceptable)	4	0

^aClusPro ranking of the docking poses, with lower numbers indicating better predictions. DockQ values, which assess docking pose quality on a scale from 0 to 1, where high-quality models are defined by $\text{DockQ} \geq 0.80$, medium-quality models by $0.80 > \text{DockQ} \geq 0.49$, acceptable-quality models by $0.49 > \text{DockQ} \geq 0.23$, and incorrect models by $\text{DockQ} < 0.23$. MLCE indicates the number of HER2 residues in a predicted patch that are actually involved in binding the affitin in the docking model, for the four models HER2–Affitin_1 and HER2–Affitin_2.

energetically unoptimized, making them more likely to tolerate mutations or interact with other molecules.

In contrast, the DockQ score is a metric used to assess the quality of protein–protein docking models, based on geometrical features rather than energetics features. It integrates three established measures, Fnat (fraction of native contacts), l-RMSD (ligand root-mean-square deviation), and i-RMSD (interface root-mean-square deviation), into a single score, with higher scores indicating better quality.

Since the two methods complement each other, providing a more robust framework for evaluating the models of the complexes, the combined use of DockQ and MLCE can strengthen the conclusions that can be drawn. Moreover, it is worth noting that the ClusPro score can be included as a third criterium to determine the most probable poses.

Table 2 shows the DockQ values and the number of HER2 residues belonging to a patch that are at the same time involved in the binding of the affitin in the docking model for the four models HER2–Affitin_1 and the four models HER2–Affitin_2.

Considering the HER2–Affitin_1 docking models, the results show that for three of the four poses, there is little or no overlap with the MLCE patches: model #0-red and model #7-orange match only 3 and 4 residues belonging to a patch, respectively; model #4-green has no match at all. Model #1-yellow totally overlaps to the patch (consisting of 27 HER2 residues, shown in violet in Figure 3) instead, but it also has the lowest DockQ value overall (0.27). However, based on previous results,¹⁸ small differences (<0.1) in DockQ values are not considered significant, as these values lie often in a narrow range, thus not being always remarkably useful for assessing the actual quality of the models. It was therefore concluded that model #1-yellow is the most likely, followed by model #0-red, which has the highest DockQ value (0.45) and is the first in the ClusPro ranking.

Similar considerations can be made for the HER2–Affitin_2 models. Models #2-orange and #3-green have no overlap with the patches; model #0-red shows only a partial match with a patch (9 residues). Model #1-yellow totally overlaps with the violet patch in Figure 3, although it has the second lowest DockQ value in the series (0.29). As it was stated for the HER2–Affitin_1 docking poses, it can be concluded that also for the HER2–Affitin_2 pair, model #1-yellow might be the most probable, followed by model #0-red, which has the

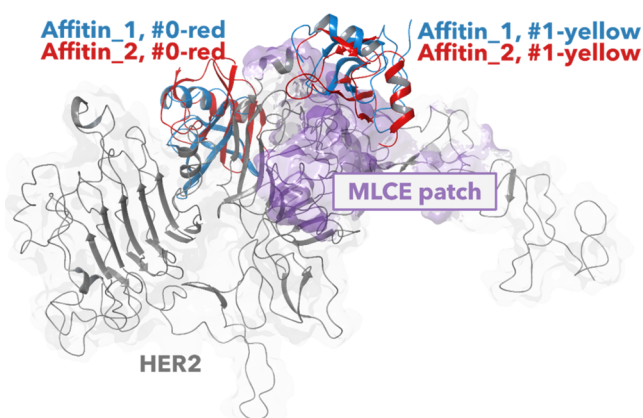


Figure 3. Superimposition of HER2–Affitin_1 and HER2–Affitin_2 docking models #1-yellow and #0-red. HER2 is shown in gray, the MLCE patch in violet, and Affitin_1 and Affitin_2 in blue and red, respectively. The list of HER2 residues in contact with the affitins in the poses is shown in Supporting Table S2.

second highest DockQ value (0.37) and is the first one in the ClusPro ranking.

The most likely models for the HER2–Affitin_1 and HER2–Affitin_2 pairs, i.e., the #1-yellow models in both cases, show a high degree of overlap between the two affitins. The same is observed for the two second most likely models, i.e., models #0-red. The superimposition of these models is shown in Figure 3. In Supporting Table S2, the list of HER2 residues in contact with the affitins in the #1-yellow and #0-red poses is reported.

The overlap between the two #1-yellow models, and between the two #0-red models, is in accordance with the experimental evidence that Affitin_1 and Affitin_2 compete for the same binding site, i.e., epitope, on the HER2 surface (Bracco Imaging S.p.A. internal communication).

As shown in Table 2, the DockQ scores for most docking poses fall within the acceptable-quality range or lower. This suggests that while these poses retain essential characteristics for potential binding, they may not maintain the predicted pose consistently throughout the simulation time.

Similar results have been obtained in a previous study we conducted on seven complexes available in the Protein Data Bank and consisting of different mutated affitins and their protein partners.¹⁸ Briefly, we observed that the MD simulations carried out for the crystallographic structures

never led to high-quality DockQ values (≥ 0.80), while only two out of seven fell in the medium-quality area. Moreover, from the simulations performed on native docking poses, i.e., poses very similar to the crystallographic structures, only three (out of seven) medium-quality DockQ values (≥ 0.49) were obtained, while the remaining were in the acceptable-quality range.

Several factors could explain this outcome. First, the docking poses generated by established algorithms are approximations that might not fully represent the most stable or optimal configurations of the complexes. Additionally, the flexibility of proteins during MD simulations can lead to significant variations in pose stability, as the conformational landscape of the complexes is more extensively explored. As a result, the average DockQ score derived from MD, which uses as reference the initial docking pose, may reflect a wide range of conformational states, resulting in lower scores. Furthermore, the integration of dynamic evaluations in the DockQ assessment process may reduce the influence of individual high-quality poses, decreasing the impact on the final score.

These results highlight the complexity of modeling protein–protein interactions and the need for further refinement of both protein–protein docking methodologies and simulation protocols.

Comparison of the Docking Models with the Map of HER2 Interactors. As previously mentioned, the results of a modeling procedure require careful evaluation and verification. They can, however, be helpful to guide experimental tests, which are necessary to validate what is obtained through the *in silico* procedure. Among the experimental tests, competitive binding assays measure the binding affinity of a ligand toward a target, in the presence of a different ligand whose binding mode to the same target is known. In this perspective, the structures of complexes available in the PDB involving HER2 and different protein partners were collected; these were compared by superimposing the HER2 chains in the complexes considered onto each other. The resulting “map” of HER2 interactors is shown in [Supporting Figure S8](#): 14 protein partners, including mAbs fragments (Fab, scFv, sdAb) and antibody mimetics, bind HER2 to different, yet sometimes overlapping epitopes mainly located in domains I, II, and IV.

HER2 structures in complexes with the protein partners were superimposed on HER2 structures in the #1-yellow docking models. The eventual overlap between Affitin_1 and Affitin_2, and the known protein partners, was then visually inspected. [Figure 4](#) shows that an overlap does exist between the docking models #1-yellow and the HER2 partners included in PDB entries 3MZW¹¹ and 3N85,³⁵ of which the former is an affibody, i.e., an antibody mimetic, and the latter is a Fab.

This observation suggests that the identified area is indeed a plausible binding site of Affitin_1 and Affitin_2, supporting its potential as a target for further experimental validation.

CONCLUSIONS

The present study concerns the prediction of the structures of the complexes that Affitin_1 and Affitin_2, which can be used as molecular vectors to design *in vivo* imaging probes, form with the receptor HER2, an important target for therapeutic and diagnostic purposes.

The first part of the study focused on the impact that the introduction of mutations in the amino acid sequence of wild-type affitin Sac7d has on the fold. This was achieved by building the homology models of Affitin_1 and Affitin_2 and

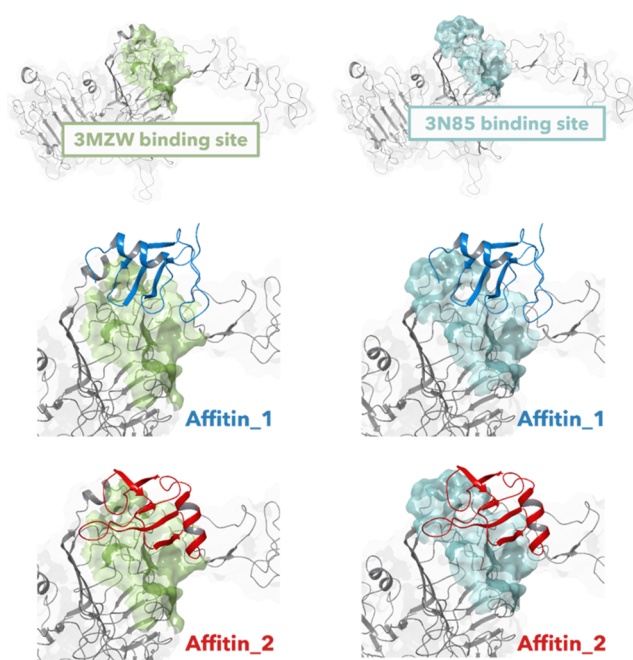


Figure 4. Comparison of HER2 known binding sites with Affitin_1 and Affitin_2 #1-yellow docking poses. Top: HER2 binding sites of protein partners are from PDB IDs 3MZW (left, light green) and 3N85 (right, cyan). Middle: comparison of Affitin_1 docking pose #1-yellow with the 3MZW (left) and the 3N85 (right) binding sites. Bottom: comparison of Affitin_2 docking pose #1-yellow with the 3MZW (left) and the 3N85 (right) binding sites. The list of HER2 residues that interact with both the protein partners from complexes 3MZW and 3N85 and the affitins is shown in [Supporting Table S3](#).

performing MD simulations. Analysis of the MD trajectories showed that the fold is overall conserved, indicating that the engineered affitins retain structural stability similar to that of the wild type.

The second part of the study dealt with predicting the binding modes of Affitin_1 and Affitin_2 with the HER2 receptor. The experimental information at our disposal, i.e., the lack of competition with the mAbs trastuzumab and pertuzumab, and the awareness that the affitin residues responsible for the interaction with HER2 are the ones mutated with respect to the wild-type affitin, was used to guide the docking calculations. In this way, the same four possible binding areas were identified for both of the affitins. The best scoring models belonging to each of these areas were selected for further evaluation with a DockQ-MLCE-based procedure that was validated in a previous work on affitin–protein complexes with experimentally known structures. The analysis of these 8 poses (4 for Affitin_1 and 4 for Affitin_2) led to the conclusion that, for both affitins, the most likely poses are the #1-yellow ones. This suggests that Affitin_1 and Affitin_2 should bind HER2 in the same area, which aligns with the experimental data, indicating competition for the same HER2 epitope.

In the last part, we demonstrated how the results of the modeling procedure can guide competitive binding assays. By superimposing the HER2 structures in the complexes with the HER2 known protein partners onto the most likely docking models, we identified an overlap between the affitins and the protein partners in PDB entries 3MZW and 3N85 (an affibody and a Fab, respectively). This indicates that competitive binding assays with these two partners could be performed,

thus reducing the number of experiments needed to unambiguously determine the structures of the HER2–Affitin_1 and HER2–Affitin_2 complexes.

In conclusion, this study combined experimental information with a computational modeling procedure at two stages. First, experimental data guided the docking predictions. Second, we showed how the results of such predictions can, in turn, be used to perform “targeted” competitive binding assays, thereby reducing the number of HER2 partners to be considered for such tests, significantly enhancing the efficiency of experimental investigations. The identified overlap with known protein partners supports the potential of the predicted binding sites as promising interaction regions, providing a strong foundation for future experimental investigations. Additionally, this study underscores the value of integrating computational and experimental methodologies to streamline the process of validating molecular interactions, which is crucial for the development of therapeutic and diagnostic tools. Finally, although this approach was designed for the HER2 target, it is a versatile method that can be easily generalized to other targets.

■ ASSOCIATED CONTENT

SI Supporting Information

The Supporting Information is available free of charge at <https://pubs.acs.org/doi/10.1021/acsomega.4c07317>.

Alignment of Sac7d, Affitin_1 and Affitin_2 sequences (Figure S1); structures of Affitin_1 and Affitin_2 (Figure S2); structure of the complex of HER2 with the monoclonal antibodies (Figure S3); centrotypes obtained from the MD simulation of the HER2–Trastuzumab complex (Figure S4); root-mean-square deviations of affitins backbone atoms (Figure S5); root-mean-square fluctuations of affitins backbone atoms (Figure S6); superimposition of all the HER2–affitins docking poses (Figure S7); overview of the protein partners of the HER2 receptor (Figure S8); secondary structure elements of affitins (Table S1); list of HER2 residues in the yellow and red docking poses (Table S2); list of HER2 residues in contact with the known protein partners and the yellow docking poses (Table S3); details on the molecular dynamics simulations of the affitins (Text S1); details on the molecular dynamics simulations of the docking poses (Text S2); and Supporting References (PDF)

■ AUTHOR INFORMATION

Corresponding Author

Anna Ranaudo – Department of Earth and Environmental Sciences, University of Milano-Bicocca, 20126 Milan, Italy; orcid.org/0000-0002-8733-7938; Email: anna.ranaudo@unimib.it

Authors

Ugo Cosentino – Department of Earth and Environmental Sciences, University of Milano-Bicocca, 20126 Milan, Italy; orcid.org/0000-0003-3671-8009
Claudio Greco – Department of Earth and Environmental Sciences, University of Milano-Bicocca, 20126 Milan, Italy; orcid.org/0000-0001-9628-7875

Giorgio Moro – Department of Biotechnology and Biosciences, University of Milano-Bicocca, 20126 Milan, Italy; orcid.org/0000-0001-7380-4411

Alessandro Maiocchi – Bracco S.p.A, 20134 Milan, Italy
Elisabetta Moroni – Institute of Chemical Sciences and Technologies “G. Natta”, National Research Council of Italy, 20131 Milan, Italy; orcid.org/0000-0002-7705-7457

Complete contact information is available at:

<https://pubs.acs.org/10.1021/acsomega.4c07317>

Author Contributions

The manuscript was written through contributions of all authors. All authors have given approval to the final version of the manuscript.

Notes

The authors declare no competing financial interest.

■ ACKNOWLEDGMENTS

The computations were carried out on high-performance computing resources provided by CINECA as part of the agreement with the University of Milano-Bicocca.

■ ABBREVIATIONS

DSPP, define secondary structure of proteins; Fab, antigen-binding fragments; HER2, human epidermal growth-factor receptor 2; MLCE, matrix of local coupling energies; RMSD, root-mean-square deviations; RMSF, root-mean-square fluctuations; scFv, single-chain variable fragments; sdAb, single domain antibodies

■ REFERENCES

- (1) Bateman, A.; Martin, M.-J.; Orchard, S.; Magrane, M.; Ahmad, S.; Alpi, E.; Bowler-Barnett, E. H.; Britto, R.; Bye-A-Jee, H.; Cukura, A.; Denny, P.; Dogan, T.; Ebenezer, T.; Fan, J.; Garmiri, P.; da Costa Gonzales, L. J.; Hatton-Ellis, E.; Hussein, A.; Ignatchenko, A.; Insana, G.; Ishtiaq, R.; Joshi, V.; Jyothi, D.; Kandasamy, S.; Lock, A.; Luciani, A.; Lugaric, M.; Luo, J.; Lussi, Y.; MacDougall, A.; Madeira, F.; Mahmoudy, M.; Mishra, A.; Moulang, K.; Nightingale, A.; Pundir, S.; Qi, G.; Raj, S.; Raposo, P.; Rice, D. L.; Saidi, R.; Santos, R.; Speretta, E.; Stephenson, J.; Tootoo, P.; Turner, E.; Tyagi, N.; Vasudev, P.; Warner, K.; Watkins, X.; Zaru, R.; Zellner, H.; Bridge, A. J.; Aimo, L.; Argoud-Puy, G.; Auchincloss, A. H.; Axelsen, K. B.; Bansal, P.; Baratin, D.; Batista Neto, T. M.; Blatter, M.-C.; Bolleman, J. T.; Boutet, E.; Breuza, L.; Gil, B. C.; Casals-Casas, C.; Echioukh, K. C.; Coudert, E.; Cucho, B.; de Castro, E.; Estreicher, A.; Famiglietti, M. L.; Feuermann, M.; Gasteiger, E.; Gaudet, P.; Gehant, S.; Gerritsen, V.; Gos, A.; Gruaz, N.; Hulo, C.; Hyka-Nouspikel, N.; Jungo, F.; Kerhornou, A.; Le Mercier, P.; Lieberherr, D.; Masson, P.; Morgat, A.; Muthukrishnan, V.; Paesano, S.; Pedruzzi, I.; Pilbout, S.; Pourcel, L.; Poux, S.; Pozzato, M.; Pruess, M.; Redaschi, N.; Rivoire, C.; Sigrist, C. J. A.; Sonesson, K.; Sundaram, S.; Wu, C. H.; Arighi, C. N.; Arminski, L.; Chen, C.; Chen, Y.; Huang, H.; Laiho, K.; McGarvey, P.; Natale, D. A.; Ross, K.; Vinayaka, C. R.; Wang, Q.; Wang, Y.; Zhang, J. UniProt: The Universal Protein Knowledgebase in 2023. *Nucleic Acids Res.* **2023**, *51* (D1), D523–D531.
- (2) Cho, H. S.; Mason, K.; Ramyar, K. X.; Stanley, A. M.; Gabelli, S. B.; Denney, D. W.; Leahy, D. J. Structure of the Extracellular Region of HER2 Alone and in Complex with the Herceptin Fab. *Nature* **2003**, *421* (6924), 756–760.
- (3) Wang, J.; Xu, B. Targeted Therapeutic Options and Future Perspectives for HER2-Positive Breast Cancer. *Signal Transduct. Target. Ther.* **2019**, *4* (1), 34.
- (4) Slamon, D. J.; Leyland-Jones, B.; Shak, S.; Fuchs, H.; Paton, V.; Bajamonde, A.; Fleming, T.; Eiermann, W.; Wolter, J.; Pegram, M.; Baselga, J.; Norton, L. Use of Chemotherapy plus a Monoclonal

- Antibody against HER2 for Metastatic Breast Cancer That Over-expresses HER2. *N. Engl. J. Med.* **2001**, *344* (11), 783–792.
- (5) Barthélémy, P.; Leblanc, J.; Goldbarb, V.; Wendling, F.; Kurtz, J.-E. Pertuzumab: Development beyond Breast Cancer. *Anticancer Res.* **2014**, *34* (4), 1483–1491.
- (6) Nami, B.; Maadi, H.; Wang, Z. Mechanisms Underlying the Action and Synergism of Trastuzumab and Pertuzumab in Targeting HER2-Positive Breast Cancer. *Cancers* **2018**, *10* (10), 342.
- (7) Franklin, M. C.; Carey, K. D.; Vajdos, F. F.; Leahy, D. J.; de Vos, A. M.; Sliwkowski, M. X. Insights into ErbB Signaling from the Structure of the ErbB2-Pertuzumab Complex. *Cancer Cell* **2004**, *5* (4), 317–328.
- (8) Hao, Y.; Yu, X.; Bai, Y.; McBride, H. J.; Huang, X. Cryo-EM Structure of HER2-Trastuzumab-Pertuzumab Complex. *PLoS One* **2019**, *14* (5), No. e0216095.
- (9) Akbari, V.; Chou, C. P.; Abedi, D. New Insights into Affinity Proteins for HER2-Targeted Therapy: Beyond Trastuzumab. *Biochim. Biophys. Acta, Rev. Cancer* **2020**, *1874* (2), No. 188448.
- (10) Yu, X.; Yang, Y.-P. P.; Dikici, E.; Deo, S. K.; Daunert, S. Beyond Antibodies as Binding Partners: The Role of Antibody Mimetics in Bioanalysis. *Annu. Rev. Anal. Chem.* **2017**, *10* (1), 293–320.
- (11) Eigenbrot, C.; Ultsch, M.; Dubnovitsky, A.; Abrahmsen, L.; Hard, T. Structural Basis for High-Affinity HER2 Receptor Binding by an Engineered Protein. *Proc. Natl. Acad. Sci. U.S.A.* **2010**, *107* (34), 15039–15044.
- (12) Jost, C.; Schilling, J.; Tamaskovic, R.; Schwill, M.; Honegger, A.; Plücker, A. Structural Basis for Eliciting a Cytotoxic Effect in HER2-Overexpressing Cancer Cells via Binding to the Extracellular Domain of HER2. *Structure* **2013**, *21* (11), 1979–1991.
- (13) Kim, T. Y.; Cha, J. S.; Kim, H.; Choi, Y.; Cho, H. S.; Kim, H. S. Computationally-Guided Design and Affinity Improvement of a Protein Binder Targeting a Specific Site on HER2. *Comput. Struct. Biotechnol. J.* **2021**, *19*, 1325–1334.
- (14) Robinson, H.; Gao, Y.-G.; McCrary, B. S.; Edmondson, S. P.; Shriner, J. W.; Wang, A. H.-J. The Hyperthermophile Chromosomal Protein Sac7d Sharply Kinks DNA. *Nature* **1998**, *392* (6672), 202–205.
- (15) Goux, M.; Becker, G.; Gorré, H.; Dammico, S.; Desselle, A.; Egrise, D.; Leroi, N.; Lallemand, F.; Bahri, M. A.; Doumont, G.; Plenevaux, A.; Cinier, M.; Luxen, A. Nanofitin as a New Molecular-Imaging Agent for the Diagnosis of Epidermal Growth Factor Receptor Over-Expressing Tumors. *Bioconjugate Chem.* **2017**, *28* (9), 2361–2371.
- (16) Reitano, E.; Maiocchi, A.; Poggi, L.; Crivellini, F.; Huet, S.; Cinier, M.; Kitten, O. WO2021122726 - Anti-HER2 Polypeptides Derivatives as New Diagnostic Molecular Probes. WO2021/122726, 2021. https://patentscope.wipo.int/search/en/detail.jsf?docId=WO2021122726&_cid=P22-LLNG30-75303-2.
- (17) Reitano, E.; Maiocchi, A.; Poggi, L.; Crivellini, F.; Huet, S.; Cinier, M.; Kitten, O. WO122729 - Anti-HER2 Polypeptides Derivatives as New Diagnostic Molecular Probes. WO2021/122729, 2021.
- (18) Ranaudo, A.; Cosentino, U.; Greco, C.; Moro, G.; Bonardi, A.; Maiocchi, A.; Moroni, E. Evaluation of Docking Procedures Reliability in Affitins-Partners Interactions. *Front. Chem.* **2022**, *10* (December), No. 1074249.
- (19) Basu, S.; Wallner, B. DockQ: A Quality Measure for Protein-Protein Docking Models. *PLoS One* **2016**, *11* (8), No. e0161879.
- (20) Tiana, G.; Simona, F.; De Mori, G. M.; et al. Understanding the Determinants of Stability and Folding of Small Globular Proteins from Their Energetics. *Protein Sci.* **2004**, *13* (1), 113–124.
- (21) Morra, G.; Colombo, G. Relationship between Energy Distribution and Fold Stability: Insights from Molecular Dynamics Simulations of Native and Mutant Proteins. *Proteins: Struct., Funct., Genet.* **2008**, *72* (2), 660–672.
- (22) Scarabelli, G.; Morra, G.; Colombo, G. Predicting Interaction Sites from the Energetics of Isolated Proteins: A New Approach to Epitope Mapping. *Biophys. J.* **2010**, *98* (9), 1966–1975.
- (23) Genoni, A.; Morra, G.; Colombo, G. Identification of Domains in Protein Structures from the Analysis of Intramolecular Interactions. *J. Phys. Chem. B* **2012**, *116* (10), 3331–3343.
- (24) Abraham, M. J.; Murtola, T.; Schulz, R.; Páll, S.; Smith, J. C.; Hess, B.; Lindahl, E. GROMACS: High Performance Molecular Simulations through Multi-Level Parallelism from Laptops to Supercomputers. *SoftwareX* **2015**, *1–2*, 19–25.
- (25) Oostenbrink, C.; Villa, A.; Mark, A. E.; Van Gunsteren, W. F. A Biomolecular Force Field Based on the Free Enthalpy of Hydration and Solvation: The GROMOS Force-Field Parameter Sets 53A5 and 53A6. *J. Comput. Chem.* **2004**, *25* (13), 1656–1676.
- (26) Berendsen, H. J. C.; Postma, J. P. M.; van Gunsteren, W. F.; Hermans, J. Interaction Models for Water in Relation to Protein Hydration. In *Intermolecular Forces: Proceedings of the Fourteenth Jerusalem Symposium on Quantum Chemistry and Biochemistry Held in Jerusalem, Israel, April 13–16, 1981*; Pullman, B., Ed.; Springer Netherlands: Dordrecht, 1981; pp 331–342.
- (27) Lindorff-Larsen, K.; Piana, S.; Palmo, K.; Maragakis, P.; Klepeis, J. L.; Dror, R. O.; Shaw, D. E. Improved Side-Chain Torsion Potentials for the Amber Ff99SB Protein Force Field. *Proteins: Struct., Funct., Bioinf.* **2010**, *78* (8), 1950–1958.
- (28) Jorgensen, W. L.; Chandrasekhar, J.; Madura, J. D.; Impey, R. W.; Klein, M. L. Comparison of Simple Potential Functions for Simulating Liquid Water. *J. Chem. Phys.* **1983**, *79* (2), 926–935.
- (29) Madhavi Sastry, G.; Adzhigirey, M.; Day, T.; Annabhimoju, R.; Sherman, W. Protein and Ligand Preparation: Parameters, Protocols, and Influence on Virtual Screening Enrichments. *J. Comput. Aided Mol. Des.* **2013**, *27* (3), 221–234.
- (30) Kozakov, D.; Hall, D. R.; Xia, B.; Porter, K. A.; Padhorny, D.; Yueh, C.; Beglov, D.; Vajda, S. The ClusPro Web Server for Protein–Protein Docking. *Nat. Protoc.* **2017**, *12* (2), 255–278.
- (31) Vajda, S.; Yueh, C.; Beglov, D.; Bohnuud, T.; Mottarella, S. E.; Xia, B.; Hall, D. R.; Kozakov, D. New Additions to the ClusPro Server Motivated by CAPRI. *Proteins: Struct., Funct., Bioinf.* **2017**, *85* (3), 435–444.
- (32) Desta, I. T.; Porter, K. A.; Xia, B.; Kozakov, D.; Vajda, S. Performance and Its Limits in Rigid Body Protein–Protein Docking. *Structure* **2020**, *28* (9), 1071–1081.E3.
- (33) Jandova, Z.; Vargiu, A. V.; Bonvin, A. M. J. J. Native or Non-Native Protein–Protein Docking Models? Molecular Dynamics to the Rescue. *J. Chem. Theory Comput.* **2021**, *17* (9), S944–S954.
- (34) Méndez, R.; Leplae, R.; De Maria, L.; Wodak, S. J. Assessment of Blind Predictions of Protein–Protein Interactions: Current Status of Docking Methods. *Proteins: Struct., Funct., Bioinf.* **2003**, *52* (1), 51–67.
- (35) Fisher, R. D.; Ultsch, M.; Lingel, A.; Schaefer, G.; Shao, L.; Birtalan, S.; Sidhu, S. S.; Eigenbrot, C. Structure of the Complex between HER2 and an Antibody Paratope Formed by Side Chains from Tryptophan and Serine. *J. Mol. Biol.* **2010**, *402* (1), 217–229.